

A robust assessment of the local anisotropy of the Hubble constant

Yves-Henri Sanejouand*

Faculté des Sciences et des Techniques, Nantes, France.

February 12th, 2024

Abstract

Magnitude predictions of Λ CDM, as parametrized by the Planck collaboration, are not consistent with the supernova data of the whole Pantheon+ sample even when, in order to take into account the uncertainty about its value, the Hubble constant is adjusted. This is a likely consequence of the increase of the number of low-redshift supernovae in the Pantheon+ sample, with respect to previous such samples. Indeed, when supernovae at redshifts below 0.035 are ignored, with $H_0 = 73.4 \text{ km}\cdot\text{s}^{-1}\cdot\text{Mpc}^{-1}$, Λ CDM predictions become consistent with Pantheon+ data. Interestingly, this is also the case when subsets of low-redshift supernovae roughly centered on the direction of the CMB dipole are considered, together with high-redshift ones, at least when CMB and peculiar velocities corrections are taken into account for the redshifts. These results seem robust, since they are also obtained with a simple, single-parameter tired-light model.

Keywords: Homogeneity scale, Supernovae Ia, Luminosity distance, Λ CDM, Linear-coasting models, Tired-light models.

Introduction

Since the seminal work of Einstein [1], most cosmological models have been based upon the hypothesis that the Universe is homogeneous [2, 3]. However, following the discovery that many, then so-called nebulae, are galaxies like our own [4], it has been

realized that the neighborhood of the Milky Way is highly structured, with both large voids [5, 6, 7] and superclusters of galaxies [8, 9].

Since, on large scales, the homogeneity ansatz has nowadays been well confirmed [10, 11, 12], a distance threshold above which the observable Universe is indeed nearly homogeneous must exist. Such a homogeneity scale has been found around $70 h^{-1} \text{ Mpc}$ [13, 14, 15], with an upper limit of $260 h^{-1} \text{ Mpc}$ [16], that is, at a redshift between 0.02 and 0.09.

On the other hand, a local anisotropy of the Hubble flow has been noticed [17, 18], which could be a consequence of the way matter is distributed in the vicinity of the Milky Way [19, 20, 21, 22].

In the present study, directions in the sky where the Hubble flow is quiet [23, 24], that is, where Λ CDM predictions are consistent with both low and high-redshift supernova data, were looked for. In order to assess the robustness of this analysis, consistency with the predictions of other, non-standard, models was also considered.

Supernova data

Equatorial coordinates, corrected B band magnitudes (mBcorr), heliocentric, CMB corrected, and hubble diagram redshifts (zHD), that is, redshifts with both CMB and peculiar velocities corrections, of the 1542 supernovae Ia of the Pantheon+ sample [25] were retrieved from the PantheonPlusSh0es page of the github webserver¹. Note that the magnitude of 127 supernovae was measured several

*yves-henri.sanejouand@univ-nantes.fr

¹<https://github.com/PantheonPlusSH0ES/DataRelease> (on april 2023).

times (up to four), for a total of 1700 measurements.

Like in other studies [12, 26], taking advantage of the large number of data available, the error on magnitude measurements at a given redshift was estimated using the standard error of the mean, $\sigma_B(z)$, of either 10 or 25 magnitude values² of supernovae at redshifts around z . Note that, in the later case, for the 68 data points thus defined, $\sigma_B(z)$ ranges between 0.015 and 0.15, with a median value of 0.03, that is, 0.1% of the median value of supernova mean magnitudes. Note also that there is a limited number of outliers in the Pantheon+ sample, namely, 89 magnitude values (0.5% of them) more than 1.5 IQR below the second or above the third quartile for their redshift bin, IQR being the interquartile range.

Mean magnitudes, $\overline{m_B}(z)$, were compared to $m_{th}(z)$, the values predicted by a given cosmological model, using the chi-squared test, that is, by evaluating the likelihood of:

$$\chi_{dof}^2 = \frac{1}{N_{dof}} \sum^{N_{dat}} \epsilon^2(z)$$

where $\epsilon(z)$, the weighted magnitude residual, is:

$$\epsilon(z) = \frac{m_{th}(z) - \overline{m_B}(z)}{\sigma_B(z)} \quad (1)$$

and where N_{dat} is the number of data points considered, N_{dof} being the number of degrees of freedom. In the present study, $N_{dof} = N_{dat} - 1$, since all models considered have a single free parameter, namely, H_0 , the Hubble constant, its value being determined by minimizing χ_{dof}^2 . Remember that χ_{dof}^2 values well above one (p-value $\ll 0.05$) mean that predictions are not consistent with data. On the other hand, χ_{dof}^2 values well below one usually mean that errors on the data ($\sigma_B(z)$) are overestimated.

Predicted magnitudes were obtained as follows:

$$m_{th}(z) = 5 \log_{10}(d_L) + 25 + M \quad (2)$$

where d_L is the luminosity distance, in Mpc, $M = -19.25$ being the fiducial absolute magnitude of supernovae Ia applicable to the Pantheon+ standardization [25].

²With a minimum of 10 values for the last redshift bin.

Cosmological models

Friedmann-Lemaitre models

Within the frame of Friedmann-Lemaitre models, the luminosity distance is given by [27]:

$$d_L = c_0(1+z) \frac{1}{\sqrt{|\Omega_k|}} S_k(\sqrt{|\Omega_k|} \int_0^z \frac{dz'}{H(z')}) \quad (3)$$

where c_0 is the speed of light, Ω_k , the curvature density parameter, and where, when the contribution of the radiation term is neglected:

$$H(z) = H_0 \sqrt{\Omega_m(1+z)^3 + \Omega_k(1+z)^2 + \Omega_\Lambda} \quad (4)$$

Ω_m and Ω_Λ being the matter and cosmological constant density parameters, respectively, while, by definition, $\Omega_m + \Omega_k + \Omega_\Lambda = 1$.

Analyses of Planck measurements of the cosmic microwave background anisotropies are consistent with Λ CDM, that is, a flat Friedmann-Lemaitre model, when $\Omega_m = 0.315 \pm 0.007$ [28] (with $\Omega_k=0$). A number of local probes have also been found consistent [29, 30] with this so-called cosmic concordance model [11]. Note however that significant tensions are still under extensive scrutiny [31, 32, 33], noteworthy as far as the value of the Hubble constant is concerned [34, 35]. This is the main reason why, in the present study, it is treated as a free parameter. Note that, in the case of luminosity distances, this single free parameter could as well be M , the absolute magnitude of supernovae Ia (see eqn 2–4).

In the second half of last century, the standard cosmological model was the Einstein–de Sitter model, another flat Friedmann-Lemaitre model where $\Omega_m=1$ ($\Omega_\Lambda=0$). In this case, according to eqn 4:

$$H(z) = H_0(1+z)^{3/2}$$

and eqn 3 becomes:

$$d_L = 2 \frac{c_0}{H_0} (1+z - \sqrt{1+z})$$

Recently, linear coasting models [36, 37] have attracted some attention. They are characterized by:

$$H(z) = H_0(1+z)$$

Thus, for a flat model with zero active mass like the $R_h=ct$ one [38, 39], eqn 3 becomes:

$$d_L = \frac{c_0}{H_0} (1+z) \ln(1+z)$$

while, for an open model, like the Dirac-Milne one [40]:

$$d_L = \frac{c_0}{H_0}(1+z) \sinh \{\ln(1+z)\}$$

Tired-light models

Soon after the Hubble-Lemaitre law was revealed [3, 41], alternative explanations were proposed [42, 43]. Noteworthy, the hypothesis that the energy of photons may decay during their travel [44] was backed by a pair of Nobel laureates [45, 46], an exponential law being assumed, likely by analogy with radioactive processes, namely:

$$h\nu_{obs} = h\nu_0 e^{-\frac{H_0}{c_0} d_T}$$

where ν_0 and ν_{obs} are, respectively, the frequency of the photons when they are emitted and when they are observed at d_T , the light-travel distance from their source, h being the Planck constant. As a consequence:

$$d_L = \frac{c_0}{H_0} \sqrt{1+z} \ln(1+z)$$

This model is hereafter coined eTL, standing for the exponential tired-light model.

Another tired-light model backed by a Nobel laureate [47] just assumes that the Hubble law has a general character [48, 49], namely, that:

$$d_T = \frac{c_0}{H_0} z$$

Thus:

$$d_L = \frac{c_0}{H_0} z \sqrt{1+z}$$

This model is hereafter coined lTL, standing for the linear tired-light model.

All models above assume that the Universe is transparent enough, so that absorption, noteworthy by grey dust [50, 51], can be safely neglected. So, let us also consider a more recent, non conservative tired-light model [12], hereafter coined ncTL, where, traveling on cosmological distances, photons are assumed to have significant chances to vanish, in such a way that:

$$n_{obs} = n_0 e^{-\sigma_o N_o d_T} \quad (5)$$

where n_0 and n_{obs} are, respectively, the number of emitted photons and the number of photons that

can be observed at a distance d_T from their source, σ_o and N_o being respectively the average cross-section and number density of obstacles.

On the other hand, assuming that, at least in the single-photon regime, the energy lost by a given photon is proportional to the surface of the wavefront associated to this photon [52, 53] that has crossed an obstacle during the travel of the photon between the source and the observer yields:

$$h\nu_{obs} = h\nu_0 \left(1 - \frac{N_t \sigma_o}{4\pi d_T^2}\right)$$

where N_t is the total number of obstacles crossed by the wavefront. Thus:

$$\frac{z}{1+z} = \frac{1}{3} \sigma_o N_o d_T \quad (6)$$

which, if it is assumed that:

$$H_0 = \frac{1}{3} c_0 \sigma_o N_o$$

is a Hubble-like law previously shown to be consistent with observational data of various origins [12, 54]. Thus, with eqn 5 and 6:

$$d_L = \frac{c_0}{H_0} \frac{z}{\sqrt{1+z}} e^{\frac{3}{2} \frac{z}{1+z}} \quad (7)$$

At variance with Friedmann-Lemaitre models [55], the above tired-light models do not predict an apparent time-dilation of all remote events. So, since it has been claimed that this phenomenon is observed in the light curves of supernovae Ia [56, 57, 58] or quasars [59], it is tempting to conclude that such tired-light models have been definitely excluded. Still, both claims have been challenged [60, 61, 62] while, in the case of long gamma-ray bursts, their observed duration does not seem to increase as a function of redshift [12, 63, 64, 65], in spite of the fact that they have been found at redshifts as high as 8.

Note however that, in the present study, alternative models were just examined in order to find at least one analytical formula for the luminosity distance able to match the high-redshift supernova data of the Pantheon+ sample.

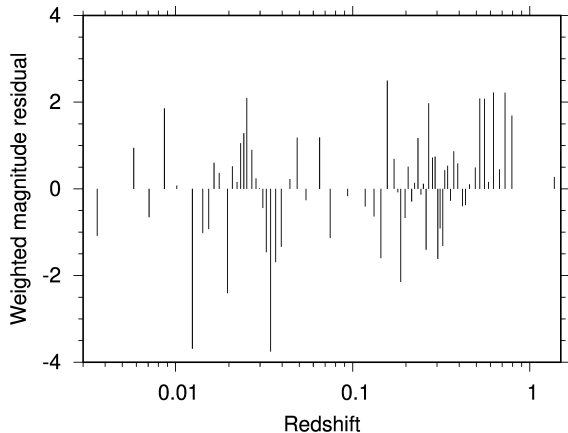


Figure 1: Difference between the magnitude predicted by Λ CDM ($\Omega_m = 0.315$) and the mean observed one, in units of the standard error of the mean magnitude of the supernovae, as a function of redshift. For each of the 68 redshift bins, 25 magnitude values are considered.

Results

Local inhomogeneity

When supernova mean magnitudes over the whole redshift range (0.004–1.38) are considered, redshifts being determined with both CMB and peculiar velocity corrections, predictions of Λ CDM (with $\Omega_m = 0.315$ [28]) are not found consistent with them ($\chi_{dof}^2 = 1.70$, p-value = 3.10^{-4}). As shown in Figure 1, $\epsilon(z)$, the weighted magnitude residual (eqn 1), has large absolute values, noteworthy around 4 for a pair of data points at $z=0.012$ and 0.034 .

On the other hand, as shown in Table 1, when supernovae at redshifts below 0.05 are ignored, while most models considered in the present study still do not prove able to match the supernova data (p-value $\ll 0.05$), a pair of them are standing out, namely, Λ CDM and ncTL.

In the former case, note that the value of the Hubble constant for which χ_{dof}^2 is minimum ($H_0 = 73.4 \text{ km}\cdot\text{s}^{-1}\cdot\text{Mpc}^{-1}$) is in perfect agreement with recent measurements of the SH0ES team ($H_0 = 73.0 \pm 1.0 \text{ km}\cdot\text{s}^{-1}\cdot\text{Mpc}^{-1}$) [66]. Note also that this χ_{dof}^2 value is over one (Table 1), suggesting that errors on the magnitudes have not been over-estimated.

Table 1: Consistency of seven models with the supernova data of the Pantheon+ sample, when supernovae at redshifts below 0.05 are ignored. For each model, H_0 is adjusted so as to minimize χ_{dof}^2 . Top: Friedman-Lemaitre models. Bottom: Tired-light models.

Model	H_0 (km/s/Mpc)	χ_{dof}^2	p-value
Λ CDM	73.4	1.29	0.08
Dirac-Milne	70.3	1.55	0.01
$R_h = ct$	69.3	2.21	0.00001
Einstein-deSitter	64.7	12.3	0 ^a
ncTL	75.1	1.23	0.12
lTL	69.6	1.85	0.0005
eTL	60.4	34.8	0 ^b

^a 10^{-83} ; ^b 10^{-279} .

Low-redshift threshold

As shown in Figure 2, Λ CDM predictions become consistent with the data from the Pantheon+ sample when supernovae at redshifts below 0.035 are ignored. Note that this threshold corresponds to the second high-value weighted magnitude residual mentioned above (Fig. 1).

Interestingly, ncTL predictions become also consistent with supernova data above approximately the same threshold (Fig. 2), even though they are poorer when the whole Pantheon+ sample is considered ($\chi_{dof}^2 = 2.49$, p-value = 2.10^{-10}).

Note that the above results are little sensitive to the way supernova redshifts are determined. Indeed, with heliocentric or CMB-corrected redshifts, a roughly identical threshold is observed, for the same pair of models.

Taken together, these results suggest that model predictions can only become consistent with the Pantheon+ data above a specific scale, which is likely to be the homogeneity one. They also illustrate the main reason why supernovae at redshifts below 0.02–0.03 are nowadays not taken into account when accurate measurements of the Hubble constant are performed [66, 67, 68].

On the other hand, with a threshold of 0.16, predictions of the $R_h = ct$, Dirac-Milne and lTL models are also found consistent with supernova data, as claimed in the case of the two former in previous studies performed with smaller samples [40, 69].

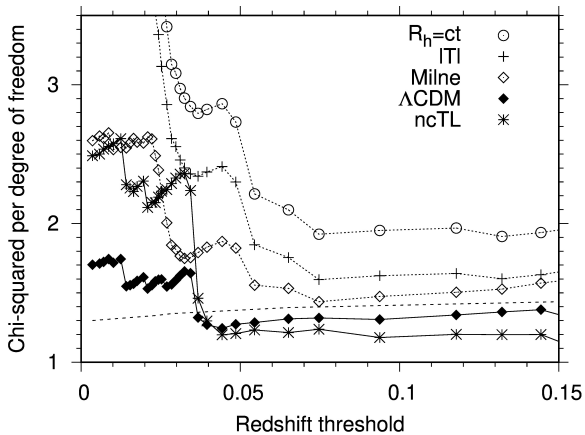


Figure 2: Chi-squared per degree of freedom as a function of the lowest supernova redshift taken into account. The dashed line indicates the value of χ^2_{dof} below which model predictions are consistent with supernova Ia mean magnitudes (p-value=0.05). Being all over 3.5, χ^2_{dof} values for the Einstein-de Sitter and eTL models are not shown.

Sky maps

Since the value of the Hubble constant seems to vary from a direction in the sky to the other [70, 71, 72] and since a dipole in the Pantheon+ data is not detected any more when supernovae at redshifts below 0.05 are ignored [73], directions in the sky along which the Hubble constant is the same at low and high-redshifts were looked for, as follows.

First, all 42 high-redshift ($z \geq 0.05$) data points considered above were kept. Second, for each of the 478 low-redshift ($z < 0.05$) supernovae of the Pantheon+ sample, the 260 magnitudes of the low-redshift supernovae that are the closest on the sky were also taken into account, with 10 magnitude values per redshift bin, so as to have, for each data set, as many points as above, with the whole Pantheon+ sample, namely, 68.

Predictions of Λ CDM and ncTL are not consistent with most of these 478 data sets, the average χ^2_{dof} being 1.47 ± 0.01 (p-value = 7.10^{-3}) and 1.78 ± 0.01 (p-value = 9.10^{-5}), respectively. However, they are found consistent (p-value ≥ 0.05) for 20% (with $H_0 = 73.4 \pm 0.1^3 \text{ km}\cdot\text{s}^{-1}\cdot\text{Mpc}^{-1}$) and 8% (with $H_0 = 74.94 \pm 0.02^3 \text{ km}\cdot\text{s}^{-1}\cdot\text{Mpc}^{-1}$) of them, respectively, meaning that, on the corresponding

³The data sets considered are not independent.

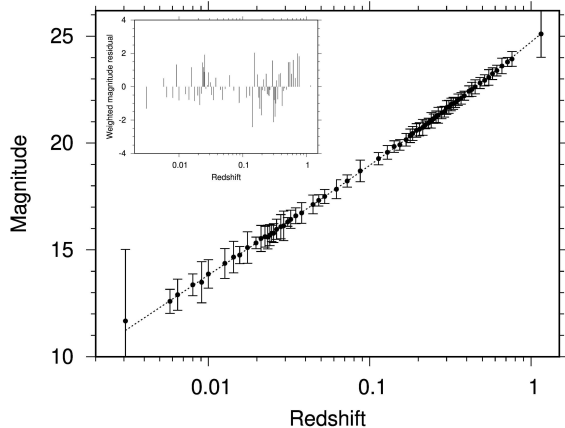


Figure 3: Mean magnitude of the supernovae Ia of the Pantheon+ sample (filled circles), as a function of redshift. Dotted line: as predicted by Λ CDM, with $\Omega_m = 0.315$ and $H_0 = 73.4 \text{ km}\cdot\text{s}^{-1}\cdot\text{Mpc}^{-1}$. For $z \geq 0.05$, each of the 42 data points is an average over 25 supernova magnitudes. For $z < 0.05$, it is an average over 10 ones, the 260 values considered being the magnitudes of the low-redshift supernovae the closest on the sky to 2016afk. Error bars are multiplied by ten for the sake of clarity. Inset: weighted magnitude residuals.

patches of the sky, the hubble flow looks quiet.

Figure 3 shows the best fit ($\chi^2_{dof} = 1.05$; p-value=0.37) over the whole redshift range thus obtained with Λ CDM, the optimized value of H_0 being $73.4 \text{ km}\cdot\text{s}^{-1}\cdot\text{Mpc}^{-1}$, that is, the value also obtained when low-redshift data are ignored (Table 1). Note that, compared to Figure 1, weighted magnitude residuals have been downsized, none of them being now over 2.4.

Interestingly, as shown in Figure 4, the low-redshift supernova data sets that are the more, or the less, consistent with both high-redshift data and either Λ CDM or ncTL largely overlap. As a matter of fact, they are almost identical. For Λ CDM, the best fit (Fig. 3) is obtained with the closest low-redshift neighbors (Fig. 4, top) of supernova 2016afk ($\alpha = 155.6^\circ$, $\delta = 15.1^\circ$) while, for ncTL, it is obtained ($\chi^2_{dof} = 1.10$; p-value=0.27) with the closest low-redshift neighbors (Fig. 4, bottom) of supernova ASASSN-16db ($\alpha = 167.4^\circ$, $\delta = 29.6^\circ$). Interestingly, the direction of the CMB dipole ($\alpha = 168^\circ$, $\delta = -7^\circ$ [74]) belongs to the area of the sky covered by both sets of super-

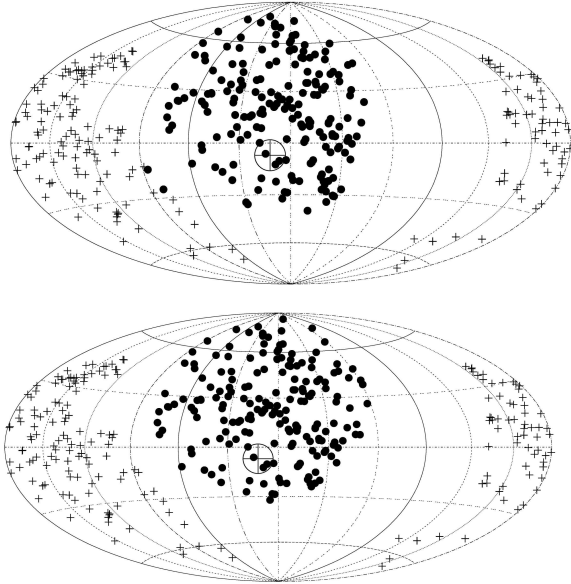


Figure 4: Location on the sky of the pair of subsets of low-redshift supernovae whose magnitudes are the more (filled circles) or the less (pluses) consistent with both the magnitudes of high-redshift supernovae and the predictions of Λ CDM (top) or ncTL (bottom), when CMB and peculiar velocities corrections are taken into account for the redshifts. Crossed circles: the direction of the CMB dipole. Hammer projections of equatorial coordinates.

novae, in line with recent results showing that H_0 is larger in an hemisphere encompassing this direction [71, 75, 76].

Note however that these later results are only obtained when CMB and peculiar velocities corrections are taken into account for the supernova redshifts. Indeed, with heliocentric redshifts, for Λ CDM, the best fit ($\chi^2_{\text{dof}} = 1.06$) is obtained with the closest low-redshift neighbors of supernova 2009ab ($\alpha = 64.2^\circ$, $\delta = 2.8^\circ$) while, for ncTL , it is obtained ($\chi^2_{\text{dof}} = 1.16$) with the closest low-redshift neighbors of supernova 2008dr ($\alpha = 332.7^\circ$, $\delta = 2.1^\circ$). On the other hand, with CMB-corrected redshifts, for both Λ CDM and ncTL , no such low-redshift data set allowing to obtain predictions consistent with the magnitudes of both low and high redshift supernovae was found, in line with the idea that the best frame of rest relative to the supernovae differ from that of the CMB [77, 78].

Conclusion

Λ CDM predictions, as parametrized by the Planck collaboration ($\Omega_m = 0.315$, $\Omega_k = 0$), become consistent with the Pantheon+ data, when the Hubble constant is adjusted, if supernovae at redshifts below 0.035 are ignored (Fig. 2), suggesting that over this threshold the homogeneity ansatz can be assumed safely. This redshift threshold corresponds to an homogeneity scale of $100 h^{-1}$ Mpc, significantly above most previous estimates [13, 14, 15], but well below upper limits [16].

With $H_0 = 73.4 \text{ km}\cdot\text{s}^{-1}\cdot\text{Mpc}^{-1}$, Λ CDM predictions are also consistent with both low and high redshift supernova data when low redshift ones come from an area of the sky whose center is roughly 30° above the direction of the CMB dipole (Fig. 4, top). This means that, in this direction, the Hubble flow looks quiet, down to $z \approx 0.003$, at least (Fig. 3).

Both results seem robust since they are also obtained with a single free parameter tired light model (eqn 7) which, interestingly, happens to be more sensitive to local inhomogeneities (Fig. 2).

Note however that a quiet Hubble flow over the whole redshift range (Fig. 3) is observed in the direction of the CMB dipole (Fig. 4) only when CMB and peculiar velocities corrections are taken into account for the supernova redshifts, underlining the need of accurate redshifts [79, 80] when studying local inhomogeneities.

Acknowledgements. I thank Carlos Bengaly, Tamara Davis, Hirokazu Fujii, Massinissa Hadjara, Georges Paturel and Diana Scognamiglio for useful suggestions and constructive comments⁴.

References

- [1] Einstein, A. (1917). Kosmologische betrachtungen zur allgemeinen Relativitatstheorie. *Sitz. Preuss. Akad. Wiss.* **1**, 142–152.
- [2] Friedman, A. (1922). Über die krümmung des raumes. *Zeitschrift für Physik* **10**(1), 377–386.
- [3] Lemaitre, G. (1927). Un Univers homogène de masse constante et de rayon croissant rendant

⁴<https://qeios.com/read/KISR8F>.

- compte de la vitesse radiale des nébuleuses extra-galactiques. *Ann. Soc. Sci. Bruxelles* **47**, 49–59.
- [4] Hubble, E.P. (1926). A spiral nebula as a stellar system: Messier 33. *Astrophysical Journal*, *63*, 236-274 (1926) **63**.
- [5] Zehavi, I., Riess, A.G., Kirshner, R.P. & Dekel, A. (1998). A local Hubble bubble from type Ia supernovae ? *Ap. J.* **503**(2), 483.
- [6] Tully, R.B., Shaya, E.J., Karachentsev, I.D., Courtois, H.M., Kocevski, D.D., Rizzi, L. & Peel, A. (2008). Our peculiar motion away from the local void. *Ap. J.* **676**(1), 184.
- [7] Keenan, R.C., Barger, A.J. & Cowie, L.L. (2013). Evidence for a ≈ 300 megaparsec scale under-density in the local galaxy distribution. *Ap. J.* **775**(1), 62.
- [8] Tully, R.B., Courtois, H., Hoffman, Y. & Pomarède, D. (2014). The Laniakea supercluster of galaxies. *Nature* **513**(7516), 71–73.
- [9] Sawala, T., Frenk, C., Jasche, J., Johansson, P.H. & Lavaux, G. (2023). Distinct distributions of elliptical and disk galaxies across the Local Supercluster as a Λ CDM prediction. *Nature Astronomy* pages 1–9.
- [10] Penzias, A.A. & Wilson, R.W. (1965). A measurement of excess antenna temperature at 4080 mc/s. *Ap. J.* **142**, 419–421.
- [11] Tegmark, M., Zaldarriaga, M. & Hamilton, A.J. (2001). Towards a refined cosmic concordance model: Joint 11-parameter constraints from the cosmic microwave background and large-scale structure. *Phys. Rev. D* **63**(4), 043007.
- [12] Sanejouand, Y.H. (2022). A framework for the next generation of stationary cosmological models. *Int. J. Mod. Phys. D* **31**(31), 2250084.
- [13] Hogg, D.W., Eisenstein, D.J., Blanton, M.R., Bahcall, N.A., Brinkmann, J., Gunn, J.E. & Schneider, D.P. (2005). Cosmic homogeneity demonstrated with luminous red galaxies. *Ap. J.* **624**(1), 54.
- [14] Sarkar, P., Yadav, J., Pandey, B. & Bharadwaj, S. (2009). The scale of homogeneity of the galaxy distribution in SDSS DR6. *Mon. Not. R. Astron. Soc. Lett.* **399**(1), L128–L131.
- [15] Ntelis, P., Hamilton, J.C., Le Goff, J.M., Burtin, E., Laurent, P., Rich, J., Tinker, J., Aubourg, E., Des Bourboux, H.D.M., Bautista, J. *et al.* (2017). Exploring cosmic homogeneity with the BOSS DR12 galaxy sample. *J. Cosmol. Astrop. Phys.* **2017**(06), 019.
- [16] Yadav, J.K., Bagla, J. & Khandai, N. (2010). Fractal dimension as a measure of the scale of homogeneity. *Mon. Not. R. Astron. Soc.* **405**(3), 2009–2015.
- [17] Davis, M. & Peebles, P. (1983). Evidence for local anisotropy of the Hubble flow. *Annual Review of Astronomy and Astrophysics* **21**(1), 109–130.
- [18] Bolejko, K., Nazer, M.A. & Wiltshire, D.L. (2016). Differential cosmic expansion and the Hubble flow anisotropy. *J. Cosmol. Astrop. Phys.* **2016**(06), 035.
- [19] Buchert, T., Kerscher, M. & Sicka, C. (2000). Back reaction of inhomogeneities on the expansion: The evolution of cosmological parameters. *Phys. Rev. D* **62**(4), 043525.
- [20] Enqvist, K. & Mattsson, T. (2007). The effect of inhomogeneous expansion on the supernova observations. *J. Cosmol. Astrop. Phys.* **2007**(02), 019.
- [21] Heinesen, A. & Macpherson, H.J. (2022). A prediction for anisotropies in the nearby Hubble flow. *J. Cosmol. Astrop. Phys.* **2022**(03), 057.
- [22] Giani, L., Howlett, C., Said, K., Davis, T. & Vagnozzi, S. (2023). An effective description of Laniakea and its backreaction: Impact on Cosmology and the local determination of the Hubble constant. *arXiv* **2311**, 00215.
- [23] Schlegel, D., Davis, M., Summers, F. & Holtzman, J.A. (1994). How unusual is the locally quiet hubble flow? *Ap. J.* **427**(2), 527–532.

- [24] Ekholm, T., Baryshev, Y., Teerikorpi, P., Hanski, M. & Paturel, G. (2001). On the quiescence of the Hubble flow in the vicinity of the Local Group-A study using galaxies with distances from the Cepheid PL-relation. *Astronomy & Astrophysics* **368**(3), L17–L20.
- [25] Scolnic, D., Brout, D., Carr, A., Riess, A.G., Davis, T.M., Dwomoh, A., Jones, D.O., Ali, N., Charvu, P., Chen, R. *et al.* (2022). The Pantheon+ analysis: the full data set and light-curve release. *Ap. J.* **938**(2), 113.
- [26] López-Corredoira, M., Melia, F., Lusso, E. & Risaliti, G. (2016). Cosmological test with the QSO Hubble diagram. *Int. J. Mod. Phys. D* **25**(05), 1650060.
- [27] Shchigolev, V. (2017). Calculating luminosity distance versus redshift in FLRW cosmology via homotopy perturbation method. *Gravitation and Cosmology* **23**, 142–148.
- [28] Aghanim, N., Akrami, Y., Ashdown, M., Aumont, J., Baccigalupi, C., Ballardini, M., Banday, A., Barreiro, R., Bartolo, N., Basak, S. *et al.* (2020). Planck 2018 results. VI. Cosmological parameters. *Astronomy & Astrophysics* **641**, A6.
- [29] Cao, S., Ryan, J. & Ratra, B. (2021). Using Pantheon and DES supernova, baryon acoustic oscillation, and Hubble parameter data to constrain the Hubble constant, dark energy dynamics, and spatial curvature. *Mon. Not. R. Astron. Soc.* **504**(1), 300–310.
- [30] Cao, S. & Ratra, B. (2022). Using lower redshift, non-CMB, data to constrain the Hubble constant and other cosmological parameters. *Mon. Not. R. Astron. Soc.* **513**(4), 5686–5700.
- [31] Di Valentino, E., Mena, O., Pan, S., Visinelli, L., Yang, W., Melchiorri, A., Mota, D.F., Riess, A.G. & Silk, J. (2021). In the Realm of the Hubble tension – a review of solutions. *Classical Quantum Gravity* **38**, 152001.
- [32] Nunes, R.C. & Vagnozzi, S. (2021). Arbitrating the s_8 discrepancy with growth rate measurements from redshift-space distortions. *Mon. Not. R. Astron. Soc.* **505**(4), 5427–5437.
- [33] Perivolaropoulos, L. & Skara, F. (2022). Challenges for Λ CDM: An update. *New Astronomy Reviews* **95**, 101659.
- [34] Wong, K.C., Suyu, S.H., Chen, G.C., Rusu, C.E., Millon, M., Sluse, D., Bonvin, V., Fassnacht, C.D., Taubenberger, S., Auger, M.W. *et al.* (2020). H0LiCOW XIII. A 2.4% measurement of H0 from lensed quasars: 5.3 σ tension between early and late-Universe probes. *Mon. Not. R. Astron. Soc.* **498**, 1420–1439.
- [35] Vagnozzi, S. (2023). Seven hints that early-time new physics alone is not sufficient to solve the Hubble tension. *Universe* **9**(9), 393.
- [36] Kolb, E.W. (1989). A coasting cosmology. *Ap. J.* **344**, 543–550.
- [37] Kaplinghat, M., Steigman, G., Tkachev, I. & Walker, T. (1999). Observational constraints on power-law cosmologies. *Phys. Rev. D* **59**(4), 043514.
- [38] Melia, F. & Shevchuk, A.S.H. (2012). The $R_h = ct$ universe. *Month. Not. Roy. Astron. Soc.* **419**(3), 2579–2586.
- [39] Melia, F. & Maier, R.S. (2013). Cosmic chronometers in the $R_h = ct$ Universe. *Month. Not. Roy. Astron. Soc.* **432**(4), 2669–2675.
- [40] Benoit-Lévy, A. & Chardin, G. (2012). Introducing the Dirac-Milne universe. *A&A* **537**, A78.
- [41] Hubble, E. (1929). A relation between distance and radial velocity among extra-galactic nebulae. *Proc. Natl. Acad. Sc. USA* **15**(3), 168–173.
- [42] Zwicky, F. (1929). On the redshift of spectral lines through interstellar space. *Proc. Nat. Acad. Sc. USA* **15**(10), 773–779.
- [43] North, J.D. (1965). *The measure of the universe. A History of modern cosmology.* Oxford University Press.
- [44] Stewart, J.Q. (1931). Nebular red shift and universal constants. *Phys. Rev.* **38**(11), 2071.
- [45] Nernst, W. (1937). Weitere prüfung der annahme eines stationären zustandes im weltall. *Zeitschrift für Physik* **106**(9-10), 633–661.

- [46] de Broglie, L. (1966). Sur le déplacement des raies émises par un objet astronomique lointain. *Comptes Rendus Acad. Sci. Paris* **263**, 589–592.
- [47] Born, M. (1954). On the interpretation of Freundlich’s red-shift formula. *Proc. Phys. Soc. A* **67**(2), 193.
- [48] Finlay-Freundlich, E. (1954). Red-shifts in the spectra of celestial bodies. *Proc. Phys. Soc. A* **67**(2), 192.
- [49] Lerner, E.J., Falomo, R. & Scarpa, R. (2014). UV surface brightness of galaxies from the local Universe to $z \approx 5$. *Int. J. Mod. Phys. D* **23**, 1450058.
- [50] Simonsen, J.T. & Hannestad, S. (1999). Can dust segregation mimic a cosmological constant? *Astron. Astrophys.* **351**(1), 1–9.
- [51] Robaina, A.R. & Cepa, J. (2007). Redshift-distance relations from type Ia supernova observations—New constraints on grey dust models. *Astron. Astrophys.* **464**(2), 465–470.
- [52] de Broglie, L. (1987). Interpretation of quantum mechanics by the double solution theory. *Annales de la Fondation Louis de Broglie* **12**(4), 1–23.
- [53] Jacques, V., Wu, E., Toury, T., Treussart, F., Aspect, A., Grangier, P. & Roch, J.F. (2005). Single-photon wavefront-splitting interference: an illustration of the light quantum in action. *The European Physical Journal D-Atomic, Molecular, Optical and Plasma Physics* **35**, 561–565.
- [54] Sanejouand, Y.H. (2014). A simple Hubble-like law in lieu of dark energy. *arXiv* **1401**, 2919.
- [55] Wilson, O.C. (1939). Possible applications of supernovae to the study of the nebular red shifts. *Ap. J.* **90**, 634.
- [56] Kim, M., Lee, J., Matheson, T., McMahon, R., Newberg, H., Pain, R. *et al.* (1996). Cosmological time dilation using type Ia supernovae as clocks. *Nucl. Phys. B* **51**, 123–127.
- [57] Leibundgut, B., Schommer, R., Phillips, M., Riess, A., Schmidt, B., Spyromilio, J., Walsh, J., Suntzeff, N., Hamuy, M., Maza, J. *et al.* (1996). Time dilation in the light curve of the distant type Ia supernova SN 1995K. *Ap. J.* **466**(1), L21–L24.
- [58] Blondin, S., Davis, T.M., Krisciunas, K., Schmidt, B., Sollerman, J., Wood-Vasey, W., Becker, A., Challis, P., Clocchiatti, A., Damke, G. *et al.* (2008). Time dilation in type Ia supernova spectra at high redshift. *Ap. J.* **682**(2), 724.
- [59] Lewis, G.F. & Brewer, B.J. (2023). Detection of the cosmological time dilation of high redshift quasars. *arXiv* **2306**, 04053.
- [60] Crawford, D.F. (2017). A problem with the analysis of type Ia supernovae. *Open Astron.* **26**(1), 111–119.
- [61] Hawkins, M. (2001). Time dilation and quasar variability. *Ap. J. letters* **553**(2), L97.
- [62] Hawkins, M. (2010). On time dilation in quasar light curves. *Mon. Not. Roy. Astron. Soc.* **405**(3), 1940–1946.
- [63] Kocevski, D. & Petrosian, V. (2013). On the lack of time dilation signatures in gamma-ray burst light curves. *Ap. J.* **765**(2), 116.
- [64] Lloyd-Ronning, N.M., Aykotalp, A. & Johnson, J.L. (2019). On the cosmological evolution of long gamma-ray burst properties. *Mon. Not. R. Astron. Soc.* **488**(4), 5823–5832.
- [65] Lloyd-Ronning, N., Johnson, J., Cheng, R.M., Luu, K., Sanderbeck, P.U., Kenoly, L. & Toral, C. (2023). On the anticorrelation between duration and redshift in gamma-ray bursts. *Ap. J.* **947**(2), 85.
- [66] Riess, A.G., Yuan, W., Macri, L.M., Scolnic, D., Brout, D., Casertano, S., Jones, D.O., Murakami, Y., Anand, G.S., Breuval, L. *et al.* (2022). A comprehensive measurement of the local value of the Hubble constant with 1 km s⁻¹ Mpc⁻¹ uncertainty from the Hubble Space Telescope and the SH0ES team. *Ap. J. letters* **934**(1), L7.

- [67] Camarena, D. & Marra, V. (2020). Local determination of the Hubble constant and the deceleration parameter. *Physical Review Research* **2**(1), 013028.
- [68] Popovic, B., Brout, D., Kessler, R. & Scolnic, D. (2023). The Pantheon+ Analysis: Forward Modeling the Dust and Intrinsic Color Distributions of Type Ia Supernovae, and Quantifying Their Impact on Cosmological Inferences. *Ap. J.* **945**(1), 84.
- [69] Wei, J.J., Wu, X.F., Melia, F. & Maier, R.S. (2015). A comparative analysis of the supernova legacy survey sample with Λ CDM and the $R_h=ct$ universe. *A. J.* **149**(3), 102.
- [70] McClure, M.L. & Dyer, C. (2007). Anisotropy in the Hubble constant as observed in the HST extragalactic distance scale key project results. *New Astronomy* **12**(7), 533–543.
- [71] Zhai, Z. & Percival, W.J. (2022). Sample variance for supernovae distance measurements and the Hubble tension. *Phys. Rev. D* **106**(10), 103527.
- [72] Aluri, P.K., Cea, P., Chingangbam, P., Chu, M.C., Clowes, R.G., Hutsemékers, D., Kochappan, J.P., Lopez, A.M., Liu, L., Martens, N.C. *et al.* (2023). Is the observable universe consistent with the cosmological principle? *Classical Quantum Gravity* **40**(9), 094001.
- [73] Sorrenti, F., Durrer, R. & Kunz, M. (2023). The Dipole of the Pantheon+ SH0ES Data. *J. Cosmol. Astrop. Phys.* **2023**(11), 054.
- [74] Hinshaw, G., Weiland, J., Hill, R., Odegard, N., Larson, D., Bennett, C., Dunkley, J., Gold, B., Greason, M., Jarosik, N. *et al.* (2009). Five-year wilkinson microwave anisotropy probe* observations: data processing, sky maps, and basic results. *The Astrophysical Journal Supplement Series* **180**(2), 225.
- [75] Krishnan, C., Mohayaee, R., Colgáin, E.Ó., Sheikh-Jabbari, M. & Yin, L. (2022). Hints of FLRW breakdown from supernovae. *Phys. Rev. D* **105**(6), 063514.
- [76] McConville, R. & Colgáin, E.Ó. (2023). Anisotropic Hubble Expansion in Pantheon+ Supernovae. *arXiv* **2304**, 02718.
- [77] Horstmann, N., Pietschke, Y. & Schwarz, D.J. (2022). Inference of the cosmic rest-frame from supernovae Ia. *Astronomy & Astrophysics* **668**, A34.
- [78] Dhawan, S., Borderies, A., Macpherson, H.J. & Heinesen, A. (2023). The quadrupole in the local Hubble parameter: first constraints using Type Ia supernova data and forecasts for future surveys. *Mon. Not. R. Astron. Soc.* **519**(4), 4841–4855.
- [79] Steinhardt, C.L., Sneppen, A. & Sen, B. (2020). Effects of supernova redshift uncertainties on the determination of cosmological parameters. *Ap. J.* **902**(1), 14.
- [80] Carr, A., Davis, T.M., Scolnic, D., Said, K., Brout, D., Peterson, E.R. & Kessler, R. (2022). The Pantheon+ analysis: Improving the redshifts and peculiar velocities of Type Ia supernovae used in cosmological analyses. *Publications of the Astronomical Society of Australia* **39**, e046.